

**Supplemental Material for: A radiofrequency voltage-controlled current source for quantum spin manipulation**

D.S. Barker,<sup>1</sup> A. Restelli,<sup>1</sup> J.A. Fedchak,<sup>2</sup> J. Scherschligt,<sup>2</sup> and S. Eckel<sup>2</sup>

<sup>1</sup>*Joint Quantum Institute, University of Maryland and National Institute of Standards and Technology*

*College Park, MD 20742, USA*

<sup>2</sup>*Sensor Science Division, National Institute of Standards and Technology*

*Gaithersburg, MD 20899, USA*

(Dated: 12 August 2020)

**Closed-loop transfer function:** Applying Kirchoff's rules to the RF VCCS circuit (see Fig. 1 in the main text) and modelling the current-feedback amplifier (CFA) as suggested in Karki<sup>S1</sup> yields:

$$\begin{aligned}
V_{\text{out}} - V_s &= I_c L_c s, \\
V_{\text{out}} - V_s &= \frac{I_p}{C_p s}, \\
V_s &= I_s R_s, \\
V_s - V_i &= I_f R_f, \\
V_i &= I_g (R_g + L_g s), \\
V_{\text{in}} - V_i &= R_i V_{\text{out}} \frac{1 + R_t C_t s}{R_t}, \\
I_c + I_p &= I_f + I_s, \\
I_g &= V_{\text{out}} \frac{1 + R_t C_t s}{R_t} + I_f.
\end{aligned} \tag{S1}$$

Here,  $s$  is the complex frequency;  $V_{\text{out}}$  is the output voltage of the CFA;  $V_s$  is the voltage across  $R_s$ ;  $V_i$  is the voltage at the inverting input of the CFA;  $V_{\text{in}}$  is the voltage at the noninverting input of the CFA;  $I_c$  is the current passing through the antenna coil  $L_c$ ;  $I_p$  is the current passing through  $C_p$ ;  $I_s$  is the current passing through  $R_s$ ;  $I_f$  is the current passing through  $R_f$ ;  $I_g$  is the current passing through  $R_g$ ; and the other symbols are defined in the main text. We have also assumed that the antenna's parasitic resistance  $R_p$  is negligible. Eliminating  $V_{\text{out}}$ ,  $V_i$ ,  $I_c$ ,  $I_p$ ,  $I_s$ ,  $I_f$ , and  $I_g$  in Eqs. S1 leads to the closed-loop transfer function

$$\begin{aligned}
H(s) &= \frac{V_s}{V_{\text{in}}} \\
&= \left[ R_s \left( R_f (R_t + R_t C_p L_c s^2) + (R_g + L_g s) (R_t + L_c s + R_t (C_p + C_t) L_c s^2) \right) \right] \\
&\quad \left/ \left[ R_f (R_g + R_i + L_g s) (1 + R_t C_t s) (R_s + L_c s + R_s C_p L_c s^2) \right. \right. \\
&\quad \left. \left. + s (R_s L_c L_g s (1 + R_t (C_p + C_t) s) + R_s L_g (R_i + R_t + R_t R_i C_t s) \right. \right. \\
&\quad \left. \left. + L_c R_i (1 + R_t C_t s) (R_s + L_g s + R_s C_p L_g s^2) \right) \right. \\
&\quad \left. \left. + R_g (R_i (1 + R_t C_t s) (R_s + L_c s + R_s C_p L_c s^2) + R_s (R_t + L_c s + R_t (C_p + C_t) L_c s^2)) \right] \right].
\end{aligned} \tag{S2}$$

The transadmittance of the RF VCCS is then

$$Y(\omega) = \frac{|H(s \rightarrow j\omega)|}{R_s}. \quad (\text{S3})$$

The linear response of the RF VCCS is given by  $Y(\omega)V_p$ , where  $V_p$  is the RF input voltage amplitude. We have found that the full transfer function of Eq. S2 does not usefully guide selection of  $R_f$ ,  $R_g$ , and  $L_g$ . Rather, we select  $R_f$  so that  $R_f + R_p + j\omega L_c$  approaches the recommended value of the feedback impedance as  $\omega$  approaches the operating bandwidth of the CFA and choose  $R_g$  to achieve the desired DC gain  $G$ .<sup>S2</sup> We then take  $C_p = 0$  and  $L_g = 0$  to reduce the number of poles in  $H(s)$ , allowing us to find that the natural frequency  $\omega_n$  and damping factor  $\zeta$  are

$$\begin{aligned} \omega_n &= \sqrt{\frac{1}{L_c C_t}} \sqrt{\frac{1 + \frac{R_f}{R_t} + \frac{R_i}{R_g} \frac{R_f + R_g}{R_t}}{1 + \frac{R_f}{R_s} + \frac{R_i}{R_g} \frac{R_s + R_f + R_g}{R_s}}}, \\ \zeta &= \frac{1}{2} \sqrt{\frac{L_c}{R_t^2 C_t}} \sqrt{\frac{R_t(R_f + R_s)}{R_s(R_f + R_t)}} \\ &\quad + \frac{1}{2} \sqrt{\frac{R_f^2 C_t}{L_c}} \sqrt{\frac{R_t R_s}{(R_f + R_t)(R_f + R_s)}}. \end{aligned} \quad (\text{S4})$$

Antennas with negligible  $R_p$  and  $L_c \gtrsim 10$  nH will exhibit underdamped poles ( $\zeta < 1$ ). To flatten the response of the RF VCCS, we add a real pole to the transfer function using  $L_g$ . When  $R_i \ll R_g$ , the pole introduced by  $L_g$  occurs at  $s = R_g/L_g$ , so  $L_g$  must be larger than  $R_g/\omega_n$  to flatten  $Y(\omega)$ .

**Open-loop transfer function:** To find the open-loop transfer function, we ground the noninverting input of the CFA and break the feedback loop at the CFA's output. The input voltage  $V_{\text{in}}$  is now applied directly to the antenna. Applying Kirchoff's rules to the open-loop circuit leads to

$$\begin{aligned} V_{\text{in}} - V_s &= I_c L_c s, \\ V_{\text{in}} - V_s &= \frac{I_p}{C_p s}, \\ V_s &= I_s R_s, \\ V_s - V_i &= I_f R_f, \\ V_i &= I_g (R_g + L_g s), \\ V_i &= -I_e R_i, \\ V_{\text{out}} &= \frac{I_e R_t}{1 + R_t C_t s}, \\ I_c + I_p &= I_f + I_s, \\ I_g &= I_e + I_f, \end{aligned} \quad (\text{S5})$$

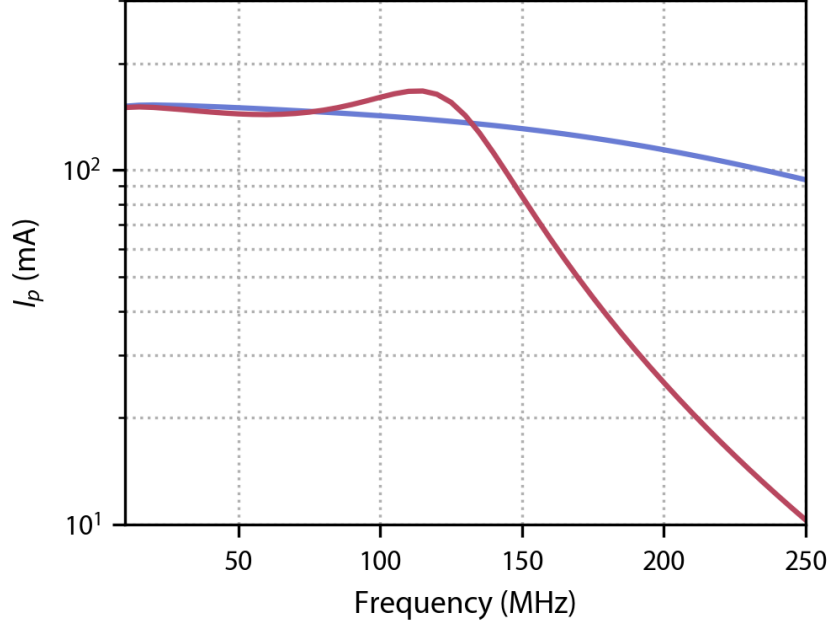


FIG. S1. Simulations of a 25 nH antenna (red) and the design from the supplemental material of Fratila et al.<sup>S3</sup> (blue). The RF input voltage for both curves is  $V_p = 127$  mV.

where  $I_e$  is the error current.<sup>S1</sup> We eliminate  $V_s$ ,  $V_i$ ,  $I_c$ ,  $I_p$ ,  $I_s$ ,  $I_f$ ,  $I_g$ , and  $I_e$  in Eqs. S5 to find the open-loop transfer function

$$\begin{aligned}
 G(s) &= \frac{V_{\text{out}}}{V_{\text{in}}} \\
 &= - \left[ R_s R_t (R_g + L_g s) (1 + C_p L_c s^2) \right] \\
 &\quad \left/ \left[ \left( 1 + C_t R_t s \right) \left( R_g (R_i R_s + L_c (R_i + R_s) s + C_p L_c R_i R_s s^2) \right. \right. \right. \\
 &\quad \left. \left. \left. + R_f (R_g + R_i + L_g s) (R_s + L_c s + C_p L_c R_s s^2) \right. \right. \right. \\
 &\quad \left. \left. \left. + s ((L_c + L_g) R_i R_s + L_c L_g (R_i + R_s) s + C_p L_c L_g R_i R_s s^2) \right) \right] \right]. \tag{S6}
 \end{aligned}$$

Once we select component values using  $H(s)$  (see above), we can compute  $G(s)$  to estimate the gain margin and phase margin of the RF VCCS.

**Low-inductance antennas:** We have simulated the performance of two low-inductance antennas. The first is an  $L_c = 25$  nH loop antenna with  $R_p = 100$  m $\Omega$  and  $C_p = 1$  pF. The second is the broadband coil design described in the supplemental material of Fratila et al.<sup>S3</sup> with  $L_c = 0.4$  nH,  $R_p = 5$   $\Omega$ , and  $C_p = 0$  pF. The results of transient simulations of the two antennas are shown in

Fig. S1. For the 25 nH antenna simulation,  $R_f = 561 \, \Omega$ ,  $R_g = 62 \, \Omega$ ,  $R_s = 8.33 \, \Omega$  (after accounting for the parallel impedance of a hypothetical spectrum analyzer),  $L_g = 130 \, \text{nH} \approx 1.3R_g/\omega_n$ . For the broadband coil simulation,  $R_f = 866 \, \Omega$ ,  $R_g = 95.3 \, \Omega$ ,  $R_s = 8.33 \, \Omega$ ,  $L_g = 0 \, \text{nH}$ . The simulated bandwidth of the RF VCCS is approximately 140 MHz for the 25 nH antenna and approximately 210 MHz for the broadband coil. We note that the THS3091 SPICE model underestimates the device bandwidth for  $G = 10$ ,<sup>S4</sup> so wider operating bandwidths may be achievable in practice.

## REFERENCES

- <sup>S1</sup>J. Karki, *Voltage Feedback Vs Current Feedback Op Amps*, Texas Instruments (1998), SLVA051.
- <sup>S2</sup>*THS309x High-voltage, Low-distortion, Current-feedback Operational Amplifiers*, Texas Instruments (2015), SLOS423H.
- <sup>S3</sup>R. M. Fratila, M. V. Gomez, S. Sýkora, and A. H. Velders, [Nature Communications](#) **5**, 3025 (2014).
- <sup>S4</sup>*THS3091 PSpice Model*, Texas Instruments (2016), Rev. A.